

Acoustic Wave propagation in a Hexagonal Surface Acoustic Wave biosensor based on LiTaO₃: A finite element study

Subramanian K.R.S. Sankaranarayanan and Venkat R. Bhethanabotla
Sensors Research Laboratory, Department of Chemical Engineering,
University of South Florida, Tampa, Florida, 33620, USA.

Abstract — We present a 3-D finite element model of a novel hexagonal SAW biosensor based on LiTaO₃ substrate. This SAW biosensor involves the use of one delay path for biological species detection whereas the other delay paths are used to simultaneously remove the non-specifically bound proteins using the acoustic streaming phenomenon, thus eliminating biofouling issues associated with other biosensors. Prior to this biosensor fabrication on any piezoelectric substrate, it is important to establish the type of waves that are generated along the various delay paths. The choice of a delay path for sensing and simultaneous cleaning application depends on the propagation characteristics of the wave generated along the crystal cut and orientation corresponding to that delay path. The frequency response as well as wave propagation characteristics along the delay path corresponding to crystal orientation with on-axis propagation along 36° YX LiTaO₃ substrate are analyzed using a coupled field FE model. Similar analysis is extended to the off-axis propagation directions corresponding to Euler rotations by 60° and -60° along the x-z plane. Our findings indicate that the on-axis direction with a significant surface shear horizontal (SH) component should be employed for biological species detection whereas the off-axis directions having mixed modes with a dominant Rayleigh wave component are most suitable for simultaneous cleaning or removal application.

Keywords – SAW; Lithium tantalate; Biosensors; Finite element method

1. INTRODUCTION

Surface acoustic wave (SAW) devices used both individually as well as in arrays find applications in chemical and biological sensing as well as in materials characterization [1]. The conventional SAW devices typically comprise of dual delay-line configurations with one delay-line used as a reference to compensate for environmental variations. Recent experimental efforts have focused on the design and fabrication of acoustic wave devices which can allow for better sensor characteristics as well as materials characterization possibilities [2]. One such novel device with a complicated transducer design is the hexagonal surface acoustic wave (SAW) sensor shown in Fig. 1. It is comprised of three different delay paths aligned to allow for generation of acoustic waves which are different in character in the different directions. It is possible to exploit the generated multiple wave modes to develop SAW devices that can serve as better chemical and biosensor elements.

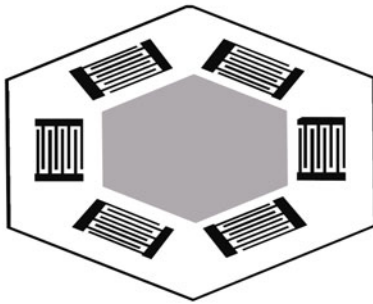


Figure 1. Schematic diagram of the hexagonal SAW device useful for chemical and bio-sensing applications.

In sensor applications, the multiple parameters extracted from the sensing film using the hexagonal SAW device can serve as multiple calibration curves and allow for a more unique and precise characterization of the concentration and type of analyte being sensed. Combined with the array concept, significantly more information can be obtained to better characterize analytes. Additionally, the hexagonal SAW device can also be employed for biological sensing. It is well known that the conventional acoustic wave devices are specific to the phase in which they operate; for example, the Rayleigh wave devices

which are suitable for vapor sensing cannot operate in the liquid environment owing to excessive attenuation [3]. If the multiple directions in which the waves are launched in the hexagonal device are different in character, then the hexagonal SAW sensor could allow the same device to be functional in both gas and liquid phases.

In one of our previous investigation, we have shown that the Rayleigh wave devices can be utilized in acoustic cleaning of nonspecifically bound proteins in biosensor applications [4-5]. With the possibility of launching shear- horizontal SAW waves in one direction and Rayleigh waves in another, the hexagonal device should serve as a better biosensor element for liquid phase applications and help to simultaneously eliminate the problems associated with biofouling which render conventional biosensors ineffective. Combined experimental and theoretical investigations to identify the best substrates and propagation directions for potential biosensing applications form the main focus of this research. Our previous theoretical and experimental investigations indicate that such a device fabricated on LiNbO₃ was better suited for material characterization than for biosensing applications [4-6].

Identifying the acoustic wave propagation characteristics on hexagonal SAW device based on several different substrates such as lithium tantalate and langasite would help us identify the best possible design for simultaneous removal of nonspecifically bound proteins and sensing utilizing Rayleigh and shear-horizontal waves. In the present work, a hexagonal SAW device based on LiTaO₃ substrate is modeled using a FE technique. The wave propagation characteristics along the three different delay paths corresponding to crystal orientation with Euler angles (0, 36, 0), (60, 36, 0) and (-60, 36, 0) respectively, are evaluated. The developed FE model utilizes anisotropic material properties in a three dimensional description of LiTaO₃ substrate. In this paper, the particle displacement and voltage profiles obtained at the output Interdigital Transducer (IDT) port as well as along the depth of the piezoelectric substrates along various locations across the three delay paths are analyzed and used to interpret the acoustic wave modes and velocity. Additionally, the response of each of the three delay lines to an applied voltage impulse is utilized to calculate its frequency response. The calculated frequency response and acoustic wave velocities are compared to those obtained experimentally and from a perturbation theory based approach.

2. THEORY

The propagation of acoustic waves in piezoelectric materials is governed by the mechanical equations of motion and Maxwell's equations for electrical behavior [7-9]. A system of four coupled wave equations for the electric potential and the three component of displacement in piezoelectric materials are solved for the piezoelectric substrate:

$$-\rho \frac{\partial^2 u_i}{\partial t^2} + c_{ijkl}^E \frac{\partial^2 u_k}{\partial x_j \partial x_l} + e_{kij} \frac{\partial^2 \phi}{\partial x_k \partial x_j} = 0 \quad (2.1)$$

$$e_{ikl} \frac{\partial^2 u_k}{\partial x_l \partial x_j} - \epsilon_{ik}^s \frac{\partial^2 \phi}{\partial x_l \partial x_k} = 0 \quad (2.2)$$

These coupled wave equations can be discretized and solved for generating displacement profiles and voltages at each element/node using the finite element method.

3. COMPUTATIONAL DETAILS

A. Model parameters

The 3-D FE model describes three two-port delay-line structures along each of the Euler direction and consists of three finger pairs in each port. The inter-digital transducer (IDT) fingers are defined on the surface of a lithium tantalate substrate and the fingers are considered as mass-less electrodes to ignore the second-order effects arising from electrode mass, to simplify computations. The periodicity of the finger pairs is 40 microns and the aperture width is 200 microns. The transmitting and receiving IDT's are spaced 130 microns or 3.25λ apart. The substrate for 36° YX LiTaO₃ was defined as 1600 microns in propagation length, 300 microns in width and 200 microns in depth. For simulating the other two propagation directions in the hexagonal biosensor, the geometry of the substrate is kept the same, whereas the crystal coordinates are rotated. To achieve this, the material properties, *i.e.*, stiffness, and piezoelectric and permittivity matrices are rotated by 60° and -60° along the x-z plane to model the off-axis directions (60, 36, 0) and (-60, 36, 0), respectively. The simulated models have a total of approx. 250000 nodes and are solved for four degrees of freedom (three displacements and voltage). The model was created to have the highest densities throughout the surface and middle of the substrate.

* Author for correspondence at email venkat@eng.usf.edu; This work was supported in part by NSF grants DGE-0221681, CHE-0722887 and ECCS-0801929, US Army Research Contract No. W81XWH-05-1-0585 and the USF Office of Research by an interdisciplinary research grant.

B. Structure excitation

Two types of analysis were carried out along each of the three delay lines: (1) An impulse input of 10 V over 1 ns was applied to study the frequency response of the device and (2) AC analysis with a 5 V peak-peak input and 100 MHz frequency was utilized to study the wave propagation characteristics.

4. RESULTS AND DISCUSSION

A. Impulse response

By applying an impulse input, the frequency response of the hexagonal SAW biosensor device was also calculated. The calculated frequency responses for an input impulse (1 ns) of 10 V for the on-axis and off-axis directions are shown in Fig. 2. The calculated device frequency along the three directions indicated that least attenuation occurs along the on-axis direction whereas higher propagation losses are observed for the off-axis directions.

The theoretical (Campbell-Jones and finite element method) and experimentally measured velocities corresponding to wave propagation along the three Euler angles are given in Table I. The SAW device frequency is directly proportional to velocity, it is expected that the frequency response would follow the order $(0, 36, 0) < (60, 36, 0) < (-60, 36, 0)$. The simulations of SAW device were performed with three IDT finger pairs. Hence, the passband obtained for the three directions is broad and the calculated device frequencies along the three directions do not show significantly different device center frequencies. The simulated device frequencies along the three directions are close to 100 MHz. Although the center frequencies are not very different, the insertion loss along the three directions varies significantly. These values for the three Euler directions are given in Table II. We find that the least attenuation occurs along the $(0, 36, 0)$ direction whereas the maximum is observed for $(-60, 36, 0)$. This indicates that the $(0, 36, 0)$ direction is most suitable for sensing applications.

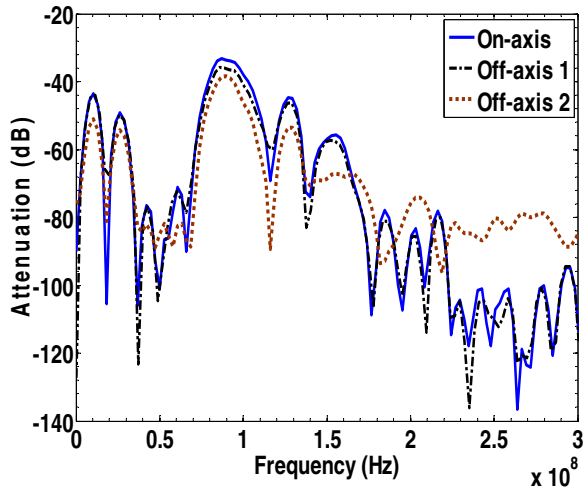


Figure 2. Calculated frequency response along the three Euler directions in the simulated hexagonal SAW biosensor. On axis corresponds to $(0, 36, 0)$ whereas off-axis-1 and off-axis-2 correspond to $(60, 36, 0)$ and $(-60, 36, 0)$ directions on a lithium tantalate substrate.

TABLE I. WAVE VELOCITIES ALONG DIFFERENT SHORTED DELAY PATHS OF LITHIUM TANTALATE

Orientation Euler angle (ϕ, θ, ψ)	Acoustic wave velocities		
	Numerical (FEM) (m/s)	Theoretical [10] (m/s)	Experimental (m/s)
$(0, 36, 0)$	4100	4039	3868 ± 148
$(60, 36, 0)$	3800	3792	3621 ± 101
$(-60, 36, 0)$	3600	3662	3593 ± 69

TABLE II. SIMULATED FREQUENCY RESPONSE OF HEXAGONAL SAW DEVICE BASED ON LiTaO_3 .

Euler direction	Simulated insertion loss
(φ, θ, ψ)	(dB)
(0, 36, 0)	33.50
(60, 36, 0)	35.00
(-60, 36, 0)	38.00

B. Response to applied AC voltage

The application of AC electrical signal on the input transducer fingers results in generation of mechanical waves which then propagate towards the output transducer fingers. The coupled field finite element model developed in the present study is able to capture the generation and propagation of SAWs on a piezoelectric substrate such as LiTaO_3 as shown in Fig. 3.

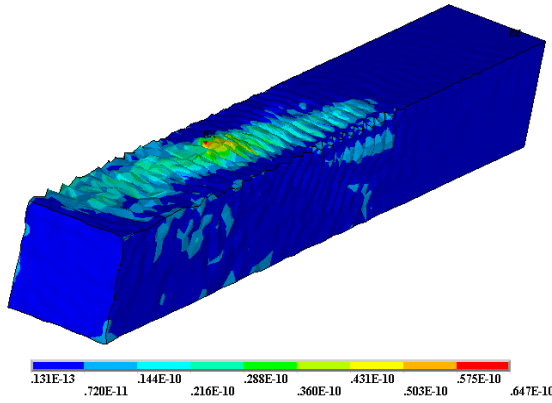


Figure 3. SAW propagation in LiTaO_3 along the (0, 36, 0) Euler direction. The displacements shown on the scale bar are in meters. It can be seen that most of the acoustic energy is confined to the surface of the piezoelectric substrate.

The displacement amplitudes of the SAWs are typically in the nanometer to angstrom range. The wave travels outside of the aperture of the IDTs located on the LiTaO_3 surface and into the substrate depth, which indicates that part of the energy is being dissipated. The generated wave also propagates in the transverse direction opposite to the receiving transducer fingers and reaches the edge of the substrate at the end of approximately 120 ns. We also observe wave reflections along the edges at longer simulation times. The generated voltage and displacement waveforms for the (0, 36, 0) delay-line configuration are shown in Fig. 4. The response to an applied electrical input was obtained at the output IDT node located 210 microns away from the input IDT fingers. Voltage profiles obtained for the three Euler directions from the AC analysis indicated that the extent of wave attenuation is different for each of the simulated crystal orientations, which is attributed to the crystal anisotropy.

Our analysis of the simulated displacement profiles indicate that the on-axis SH component of displacement at the output IDT is an order of magnitude higher than the surface normal and longitudinal components indicative of SH wave motion (Fig. 4). Thus, a SH SAW propagates along the on-axis direction (36° YX LiTaO_3) which is most suitable for biosensing application. For the off-axis direction (60, 36, 0), the surface normal and longitudinal components of displacement at the output IDT are an order of magnitude larger than the SH component indicative of wave motion which is more or less ellipsoidal. This type of wave motion corresponds closely to that of the Rayleigh mode. The displacement profiles of the other off-axis component (-60, 36, 0) showed the smallest amplitude variations amongst the three directions indicative of mixed-wave modes which are a combination of more than one wave type such as pure Rayleigh or SH modes. The wave propagation along the on-axis direction, *i.e.*, 36° YX LiTaO_3 substrate is shown in Fig. 3. At approximately 120 ns, the wave has reached the end of the substrate.

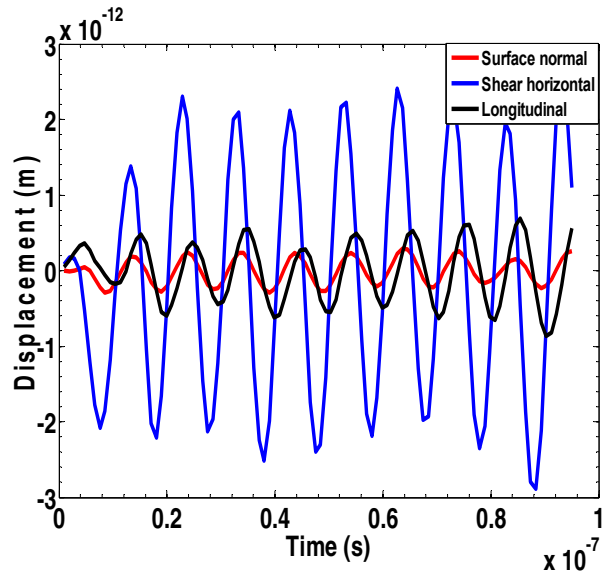


Figure 4. SH displacement component along the on-axis direction in al SAW device based on lithium tantalate.

5. CONCLUSIONS

A 3-D finite element coupled field model of a hexagonal SAW device fabricated in a LiTaO₃ substrate is developed in this work. Insights into the acoustic wave generation and propagation along the three Euler directions corresponding to the multiple propagation directions in this transducer configuration are obtained using the developed model. Our simulation results indicate that the waves propagating along the (0, 36, 0) direction have a dominant SH component whereas those propagating along the (60, 36, 0) and (-60, 30, 0) directions involve combination of multiple wave modes with a prominent surface normal displacement component. Such a device can be used for simultaneous biological species detection and non-specifically bound protein removal in SAW biosensing applications. The differences in acoustic wave modes manifest themselves in the form of differing voltage responses. We find a more attenuated voltage response at the output transducer fingers for the (60, 36, 0) and (-60, 36, 0) directions in comparison to the (0, 36, 0) direction. The calculated insertion losses for an applied impulse voltage input along the three propagation directions indicate that the waves along the (0, 36, 0) direction are less attenuated than those along the (60, 36, 0) and (-60, 36, 0) directions. The simulation results agree with those obtained using a perturbation technique based method due to Campbell-Jones as well as those observed experimentally. A 3-D FE model can thus be useful in understanding acoustic wave propagation in piezoelectric substrates. Efforts are underway to extend such simulations for hexagonal SAW devices based on other substrates such as langasite which could help identify better biosensor transducers for liquid phase applications.

ACKNOWLEDGEMENT

The authors wish to thank the Engineering Computing Center at USF for providing the computational facilities. The authors thank Samuel Ippolito and Glenn Matthews of RMIT, Melbourne and Reetu Singh of USF for useful discussions.

REFERENCES

- [1] S. Cular, V. R. Bhethanabotla, and D. W. Branch, "Hexagonal surface acoustic wave devices for enhanced sensing and material characterization," presented at IEEE Ultrasonics, Rotterdam, Netherlands, 2005.
- [2] S. Cular, D. W. Branch, V. R. Bhethanabotla, G. D. Meyer, H. G. Craighead, "Removal of nonspecifically bound proteins on microarrays using surface acoustic waves." *IEEE Sensors Journal*, vol. 8(3), pp. 314-320, 2008.
- [3] S. K. R. S. Sankaranarayanan and V. R. Bhethanabotla, "Finite element modeling of hexagonal SAW device based on LiNbO₃," *IEEE Sensors Journal*, In Press, 2008.
- [4] S. K. R. S. Sankaranarayanan, V. R. Bhethanabotla, "Design of efficient focused surface acoustic wave devices for potential microfluidic applications." *Journal of Applied Physics* vol. 103(6), pp. 064518/1-064518/17, 2008.
- [5] S. K. R. S. Sankaranarayanan, S. Cular, V. R. Bhethanabotla, and J. Babu, "Flow induced by acoustic streaming on surface-acoustic-wave devices and its application in biofouling removal: A computational study and comparisons to experiment." *Physical Review E*, vol. 77, pp. 066308/1- 066308/19, 2008.
- [6] S. Cular, S. K. R. S. Sankaranarayanan, and V. R. Bhethanabotla, "Enhancing effects of microcavities on shear-horizontal surface acoustic wave sensors: A finite element simulation study." *Applied Physics Letters*, 92(24), 244104/1-244104/3, 2008.
- [7] B. A. Auld, *Acoustic Fields and Waves in Solids.*, vol. 1-2. New York, N.Y., USA: John Wiley and Sons, 1973.

- [8] S. J. Ippolito, K. Kalantar-Zadeh, D. A. Powell, and W. Wlodarski, "A 3-dimensional finite element approach for simulating acoustic wave propagation in layered SAW devices.," presented at Ultrasonics, IEEE Symposium, 5-8 Oct. 2003.
- [9] R. Lerch, "Simulation of piezoelectric devices by two- and three-dimensional finite elements," *Ultrasonics, Ferroelectrics and Frequency Control, IEEE Transactions*, vol. 37, pp. 233 - 247, 1990.
- [10] J. J. Campbell and W. R. Jones, "A method for estimating optimal crystal cuts and propagation directions for excitation of piezoelectric surface waves.," *IEEE Transactions on Sonics and Ultrasonics*, vol. 15, pp. 209-217, 1968.